Application of Model Predictive Control Algorithm on a Hydro Turbine Governor Control

Mateo Beus, Hrvoje Pandžić
Department of Energy and Power Systems
University of Zagreb Faculty of Electrical Engineering and Computing
Zagreb, Croatia
{mateo.beus,hrvoje.pandzic}@fer.hr

***Abstract*—Operation of the most turbine governors currently in use is based on Proportional-Integral-Derivative (PID) controllers. The use of PID controllers is widespread primarily because of their extensive applicability to a variety of single-input-single-output (SISO) applications. However, classical PID controllers have disadvantages, e.g. resiliency to disturbances and uncertainties, as well as integral windup. In this regard, a controller based on the Model Predictive Control (MPC) algorithm, which is known as a Generalized Predictive Control (GPC), is developed and applied to a linearized SISO model of the hydropower plant. The response of the system with constrained GPC is compared to the classical PI controller. The main conclusion is that GPC provides better performance than the classical PI regulator.**

***Index Terms*—hydraulic turbine dynamic model, linear model, load frequency control, predictive control, turbine governors**

I. Introduction

Proportional-Integral-Derivative (PID) controllers are widespread in turbine governor applications [1]. Although they have many advantages, such as easy implementation, the main disadvantage of PID controllers is a fairly low robustness. If the system parameters cannot be precisely estimated, the designed PID controller may not be resilient to uncertainties and disturbances. Another important disadvantage of PID controller is integral windup, i.e. the process of accumulating the integral component beyond the saturation limits of actuators. More advanced types of controllers, such as controllers based on Generalized Predictive Control (GPC) algorithm, offer an alternative approach to control hydro turbines, avoiding problems associated with PID controllers.

Each turbine governor consists of two automatic controllers: a speed controller and a frequency/load controller [2]. During the start-up sequence, the speed controller is used, while the breaker is open. Once the generator is synchronized to the grid, the frequency/load controller takes over the control.

Generally speaking, the application of Model Predictive Control (MPC) for load/frequency control of hydropower plants is not widespread as for controlling thermal power plants and wind power plants. In [3], the authors analyze applicability of industrial MPC to thermal power plants. Dynamic Matrix Control (DMC) was applied on a detailed plant simulator, which is used for operator training and controllers tuning. The results have shown a great potential of MPC in terms of economical savings, reduction of pollutants and improved flexibility. In [4], the authors applied MPC to a superheater steam temperature control in the coal-fired thermal power plant. An MPC controller is compared with a classical PID controller and the obtained results showed that the steam temperature controlled by the MPC controller is more stable.

Application of MPC strategy to a large gas turbine power plant is examined in [5] order to improve plant thermal efficiency and load/frequency control capabilities. Simulation results have shown significant improvements in the frequency variations and load following capability. This has led to improvements in the overall combined cycle thermal efficiency of 1.1%. A constrained MPC-based controller for the purpose of wind turbine control was presented in [6]. The performance of the MPC controller with constraint handling is compared with the PI controller with integrator anti-windup. Simulation results have shown that MPC strategy ensures that soft constraints are satisfied to the greatest possible extent while at the same time hard constraints are not violated. The implications of formulating a single control law that governs the entire wind speed range of operation for a wind turbine are discussed in [7]. In this paper, the authors analyzed a controller based on a nonlinear MPC and that includes wind speed predictions in the prediction horizon.

The main reason why MPC is analyzed and applied more often to control of thermal power plants then to control of hydropower plants is because hydropower plants have faster dynamic behavior. In this paper the frequency/load controller is analyzed. The analyzed plant consists of a single tunnel drawing water from an upper reservoir into a manifold, which splits the flow into two groups of two penstocks. Each penstock feeds a single unit to produce electricity. Produced active power of each unit is regulated by controlling the flow of water using a guide vane at each turbine. Each turbine drives a synchronous generator and the amount of active power which is fed into the grid is regulated by the PI feedback loops or GPC, which change the guide vane angle, thus regulating the flow of water into the turbine. Unit 1 is a 4.8 MW Francis turbine, while Units 2-4 are identical 6.4 MW Francis turbines. For simulation purposes in this paper, a linearized SISO model of Unit 3 is used. A schematic representation of hydropower plant Miljacka is given in Fig. 1, while the basic parameters of the plant used to create the simulation model are listed in Table I [8].

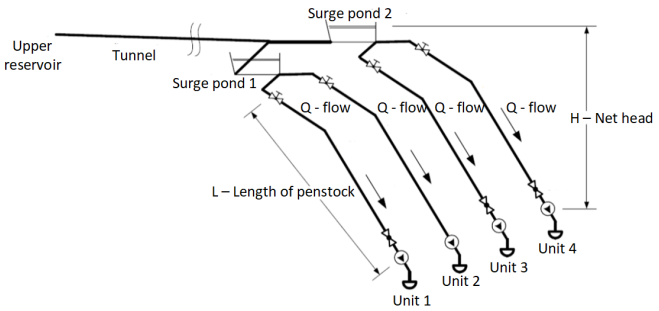

Figure 1. Schematic diagram of hydropower plant Miljacka.

TABLE I
HYDROPOWER PLANT MILJACKA PARAMETERS.

Number of units	4
Type of turbines	Francis
Rated power - Unit 1	4.8 MW
Rated power - Units 2-4	6.4 MW
Rated speed	500 rpm
Rated flow/unit	7.4 $\mathrm{m^3\,s^{-1}}$
Net head	103 m
Length of penstock	168 m
Penstock diametar	1.6 m

Nowadays, controllers for turbine governor applications are usually based on Single-Input-Single-Output (SISO) linearized models. The main issue with this is that hydropower plants are highly nonlinear systems. The two main characteristics of hydropower plants are nonlinear relationship between guide vane angle, volume flow of water and mechanical power, and Non-Minimum-Phase (NMP) behavior [9]. This implies that the parameters of the linearized model vary significantly across plant's operating range. Therefore, a fixed parameter PID structure controller can only be optimal at operating point chosen during the controller design. In this paper, GPC algorithm also uses linearized SISO model as controller's internal model and for process simulation purposes.

Main intention of this paper is to compare the proposed predictive controller with the classical PI controller using an identical SISO linearized model.

The rest of the paper is organized as follows. The plant model is explained in Section II. Unconstrained and constrained GPC algorithm formulation is explained in Section III, while simulation results and discussion are provided in Section IV. The paper is concluded in Section V.

II. SISO Plant Model

The analyzed plant model is presented in Fig. 2.

Main components of the model are:

- guide vanes and their hydraulic actuator transfer function,
- penstock transfer function,
- Francis turbine transfer function.

A simplified transfer function that describes the penstock dynamic behavior is [10]:

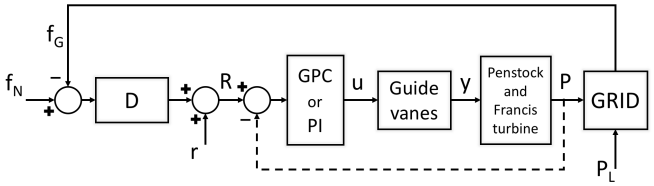

Figure 2. Subsystems of the hydropower plant.

$$\frac{\Delta h_{TC}(s)}{\Delta q_T(s)} = -T_w s, \tag{1}$$

where h_{TC} is the dynamic pressure at the end of the penstock (head), q_T is the flow of water through the turbine, T_w is the water starting constant, Δ stands for deviation, and s denotes the Laplace domain.

Francis turbine model is expressed by (2) and (3) that describe flow of water through turbine and mechanical power output [11]:

$$q_T = y\sqrt{h_{TC}} \qquad (p.u.), \tag{2}$$

$$P = A_t(q_T - q_{NL})h_{TC} - D_a y \Delta w \qquad (p.u.), \tag{3}$$

where A_t is a parameter that converts gate opening to per unit turbine power on the volt-ampere base of the generator and takes into account the turbine gain, q_{NL} is the no-load flow, D_a is turbine damping coefficient and Δw is turbine runner speed deviation.

From (2) it is clear that the turbine model is nonlinear and it is necessary to linearize the turbine model in order to obtain a linearized SISO model of the plant. Linearization of the turbine model is made by linearizing (2) and (3) in the following way:

$$\Delta q_T = k_{11}\Delta h_{TC} + k_{12}\Delta w_N + k_{13}\Delta y, \tag{4}$$

$$\Delta P = k_{21}\Delta h_{TC} + k_{22}\Delta w_N + k_{23}\Delta y, \tag{5}$$

where (6) and (7) define k_{1i} and k_{2i} coefficients ($i = 1, 2, 3$):

$$k_{11} = \frac{\partial q_T}{\partial h_{TC}}, \qquad k_{12} = \frac{\partial q_t}{\partial w_N}, \qquad k_{13} = \frac{\partial q_T}{\partial y}, \tag{6}$$

$$k_{21} = \frac{\partial P}{\partial h_{TC}}, \qquad k_{22} = \frac{\partial P}{\partial w_N}, \qquad k_{23} = \frac{\partial P}{\partial y}. \tag{7}$$

Linearization is made for the operating point:

$$\begin{aligned} h_{TC} &= 1 \qquad (p.u.), \\ w_N &= 1 \qquad (p.u.), \\ y = Y_0 &= 0.3 \quad (p.u.,). \end{aligned} \tag{8}$$

After combining (1), (4) and (5), the linearized unit's mechanical power is:

$$\Delta P = k_{22}\Delta w_N + k_{23}\Delta y - \frac{k_{21}(k_{12}\Delta w_N + k_{13}\Delta y)(-sT_w)}{-1 + k_{11}(-sT_w)}. \tag{9}$$

It is assumed that the unit is synchronized to the grid and turbine governor works in frequency/load controller mode. In case when the grid is "stiff", $\Delta w_N \approx 0$ because frequency deviation can be considered negligible.

Finally, the transfer function that describes turbine's mechanical power output as a function of the guide vane angle is expressed by:

$$\frac{\Delta P}{\Delta y} = \frac{k_{23} - (k_{13}k_{21} - k_{11}k_{23})T_w s}{1 + k_{11}T_w s}. \tag{10}$$

Additionally, guide vane opening Δy is actuated by hydraulic servo, whose transfer function is:

$$\frac{\Delta y}{u} = \frac{1}{T_a s + 1}, \tag{11}$$

where T_a is a time constant that describes dynamic of hydraulic servo actuating system and u is control signal produced by governor. Finally, the transfer function that describes SISO linearized plant model is:

$$\frac{P}{u} = \left(\frac{1}{T_a s + 1}\right)\left(\frac{k_{23} - (k_{13}k_{21} - k_{11}k_{23})T_w s}{1 + k_{11}T_w s}\right). \tag{12}$$

Classical PI governor used for simulation purposes has the following transfer function:

$$u = \left(K_p + \frac{K_i}{s}\right)(r - P), \tag{13}$$

where r is an active power set-point.

If hydropower plant provides primary reserve, active power set-point varies with respect to the grid frequency. Active power set-point change is then:

$$R = r + D(f_N - f_G), \tag{14}$$

where D presents droop characteristic, f_N is nominal frequency and f_G is grid frequency.

III. SISO GPC

A. Unconstrained SISO GPC

MPC as a control strategy has many variants and GPC is one of the most frequently used predictive control strategies, which is used in this paper.

The main idea of GPC is to include within the controller the simplest possible predictive model of the plant. The predictive model used in GPC is represented in form of transfer function. The model predicts future output of the plant based on the past and the present values of control and measured/estimated outputs of the plant if subjected to a given control input sequence. At each time step the plant's output is predicted for a specified number of samples (N) into the future, known as the prediction horizon, while control input can also be changed only for a specified number of samples (N_u) into the future, known as the control horizon. This means that the predicted error of the plant's output from a reference trajectory can be calculated. The calculations of control sequence are done in a way that an optimization problem is set up and solved. Cost function, which is as part of the optimization problem, can be set up in various ways depending on response specifications of the plant and the type of optimization problem.

Only the first value of the computed control sequence is applied to the plant at the time step for which the calculations are made. At the next time step, the output of the plant is measured/estimated, and the entire computation procedure is repeated using the receding horizon principle.

The quadratic cost function, which is used in this paper, to be minimized at each sample k is expressed by:

$$J = \begin{bmatrix} e_{\underrightarrow{k+1}}^T & e_{\underrightarrow{k+1}} \end{bmatrix} + \begin{bmatrix} \Delta u_{\underrightarrow{k}}^T & \Delta u_{\underrightarrow{k}} \end{bmatrix} \boldsymbol{W_u}, \tag{15}$$

$$e_{k+1} = r_{k+1} - y_{k+1}, \tag{16}$$

where $r_{\underrightarrow{k+1}}$ is the future reference trajectory vector, $y_{\underrightarrow{k+1}}$ is the optimal predicted output of the plant defined at prediction horizon N, Δ is the $(1 - z^{-1})$ operator, $u_{\underrightarrow{k}}$ is a control sequence and W_u positive definite weighting matrix used to penalize control effort. Vectors $r_{\underrightarrow{k+1}}$, $y_{\underrightarrow{k+1}}$ and matrix $W_u^{[N_u \times N_u]}$ are expressed by:

$$r_{\underrightarrow{k+1}} = \begin{bmatrix} r_{k+1} \\ r_{k+2} \\ \vdots \\ r_{k+N} \end{bmatrix}, y_{\underrightarrow{k+1}} = \begin{bmatrix} y_{k+1} \\ y_{k+2} \\ \vdots \\ y_{k+N} \end{bmatrix}, \boldsymbol{W_u} = \begin{bmatrix} W_u & \dots & 0 \\ \vdots & \ddots & \vdots \\ 0 & \dots & W_u \end{bmatrix}. \tag{17}$$

The discrete-time predictive model used within GPC controller in this paper is represented by using the Controlled AutoRegressive Integrated Moving Average (CARIMA) model:

$$a(z)\Delta y_k = b(z)\Delta u_k + T(z)\epsilon(z). \tag{18}$$

For convenience, as the output is measured, the prediction model uses variables of the output and input increment and assumes the best estimate of future random term $T(z)\epsilon(z) = 0$.

In (18), $b(z)$ is a polynomial that represents numerator of the transfer function, while $a(z)$ is a polynomial that represents denumerator of the transfer function:

$$a(z) = 1 + a_1 z^{-1} + \cdots + a_n z^{-n}, \quad a(z)\Delta = A(z), \tag{19}$$

$$b(z) = b_1 z^{-1} + \cdots + b_m z^{-m}. \tag{20}$$

There is no need for a disturbance estimate in this prediction model because disturbance estimate is implicit within the use of increments.

Instead of using recursion to find dependence of the output predictions upon past (or known) data and decision variables, output predictions can be found by using compact matrix/vector form:

$$y_{\underrightarrow{k+1}} = H\Delta u_{\underrightarrow{k}} + P\Delta u_{\underleftarrow{k-1}} + Q y_{\underleftarrow{k}}, \tag{21}$$

where H, P and Q matrixes are expressed as:

$$H = C_A^{-1}C_b, P = C_A^{-1}H_b, Q = C_A^{-1}. \tag{22}$$

Matrixes C_A, C_b, H_A and H_b are expressed by:

$$C_A = \begin{bmatrix} 1 & \dots & 0 & 0 \\ A_1 & 1 & 0 & 0 \\ \vdots & \ddots & \vdots & 0 \\ A_{N-1} & A_{N-2} & \dots & 1 \end{bmatrix}, \tag{23}$$

$$H_A = \begin{bmatrix} A_1 & A_2 & \cdots & A_{n-4} & A_{n-3} & \cdots & A_{n-1} & A_n \\ A_2 & A_3 & \cdots & A_{n-3} & A_{n-2} & \cdots & A_n & 0 \\ \vdots & \cdots & \cdots & A_{n-2} & A_{n-1} & \cdots & 0 & 0 \\ A_N & A_{N+1} & \cdots & A_{n-1} & A_n & \cdots & 0 & 0 \end{bmatrix}, \tag{24}$$

$$C_b = \begin{bmatrix} b_1 & 0 & 0 & 0 \\ b_2 & b_1 & 0 & 0 \\ \vdots & \ddots & \vdots & 0 \\ b_N & b_{N-1} & \dots & b_1 \end{bmatrix}, \tag{25}$$

$$H_b = \begin{bmatrix} b_2 & b_3 & \cdots & b_{m-4} & b_{m-3} & \cdots & b_{m-1} & b_m \\ b_3 & b_4 & \cdots & b_{m-3} & b_{m-2} & \cdots & b_m & 0 \\ \vdots & \cdots & \cdots & b_{m-2} & b_{m-1} & \cdots & 0 & 0 \\ b_{N+1} & b_{N+2} & \cdots & b_{m-1} & b_m & \cdots & 0 & 0 \end{bmatrix}. \tag{26}$$

In the unconstrained case, the optimal control law can be found explicitly by substituting (21) into (15), which gives the following cost function to be minimized:

$$\begin{aligned} J =& (\Delta u_k)^T (H^T H + \boldsymbol{W_u} I) \Delta u_{\underset{\rightarrow}{k}} - \\ & 2(H \Delta u_{\underset{\rightarrow}{k}})^T (r_{\underset{\longrightarrow}{k+1}} - P \Delta u_{\underset{\longleftarrow}{k-1}} - Q y_{\underset{\leftarrow}{k}}), \end{aligned} \tag{27}$$

$$u* = \min_{\Delta u_{\underset{\rightarrow}{k}}} (J). \tag{28}$$

As the cost function is quadratic and strictly positive, a unique minimum is determined by:

$$\nabla(J) = 0, \tag{29}$$

which means that in the unconstrained case the optimal control sequence can be calculated using the following equation:

$$\Delta u_{\underset{\rightarrow}{k}} = (H^T H + \boldsymbol{W_u} I)^{-1} H^T (r_{\underset{\longrightarrow}{k+1}} - P \Delta u_{\underset{\longleftarrow}{k-1}} - Q y_{\underset{\leftarrow}{k}}). \tag{30}$$

From (30) it is clear that the optimal control sequence in unconstrained case depends linearly on the future reference trajectory and past inputs/outputs.

Only the first value of the computed control sequence in (30) is applied to the plant since optimization procedure is repeated at every next time step and proposed future control increments in the current time step will be adjusted and improved in the following time steps.

Since GPC algorithm used in this paper is set up in a way that optimal input increment is calculated at each time step, the control signal sent from the controller to the actuator at time step k is computed in the following way:

$$u_k = u_{k-1} + \Delta u_k. \tag{31}$$

B. Constrained SISO GPC

Two main advantages of the MPC over the classical controllers, i.e. PID structure controllers, are following [12], [13]:

- MPC incorporates hard constraints into control law naturally during the controller design phase,
- it is relatively straightforward to extend MPC controller for SISO application to multiple input multiple output (MIMO) application.

Typical types of constraints which are usually defined within the GPC algorithm are [12], [13], [14]:

- upper and lower limits on an input $\min u \leq u_k \leq \max u \quad \forall k$,
- upper and lower limits on input rates $\min \Delta u \leq \Delta u_k \leq \max \Delta u \quad \forall k$,
- upper and lower limits on a state/output $\min y \leq y_k \leq \max y \quad \forall k$.

It is also possible to have mixed constraints, i.e. linking inputs at different samples. Constrains included in GPC algorithm are constraints on guide vane rate and amplitude. The quadratic cost function defined in (15) is used as well, in order to set up predictive controller as a quadratic programming problem subject to the control constraints $C \Delta u_{\underset{\rightarrow}{k}} \leq c$.

Matrix $C^{[4N_u \times N_u]}$, vector $c^{[4N_u \times 1]}$ and vector $\Delta u_{\underset{\rightarrow}{k}}^{[N_u \times 1]}$ are defined as follows:

$$\begin{aligned} C &= \begin{bmatrix} I \\ -I \\ I \\ -I \end{bmatrix}, \qquad \Delta u_{\underset{\rightarrow}{k}} = \begin{bmatrix} \Delta u_k \\ \Delta u_{k+1} \\ \vdots \\ \Delta u_{k+N_u-1} \end{bmatrix}, \\ c &= \begin{bmatrix} l(\max u) \\ -l(\min u) \\ l(\max \Delta u) \\ -l(\min \Delta u) \end{bmatrix}, \qquad l = \begin{bmatrix} 1 \\ 1 \\ \vdots \\ 1 \end{bmatrix}. \end{aligned} \tag{32}$$

Dimension of vector l is $[N_u \times 1]$.

C. The Predicitve Model of the Plant

GPC controller is designed using transfer function of Unit 3 of hydropower plant Miljacka defined in Section II, which consists only of guide vane and hydraulic subsystems. The predictive model of the plant with sample period $T_s = 0.25$ s has the following transfer function:

$$G(z) = \frac{0.2908z + 1.74}{z^2 - 0.7851z + 0.1494}. \tag{33}$$

The polynomials in (19) and (20) are:

$$a(z^{-1}) = 1 - 0.7851z^{-1} + 0.1494z^{-2}, \tag{34}$$

$$b(z^{-1}) = 0.2908z^{-1} + 1.74z^{-2}. \tag{35}$$

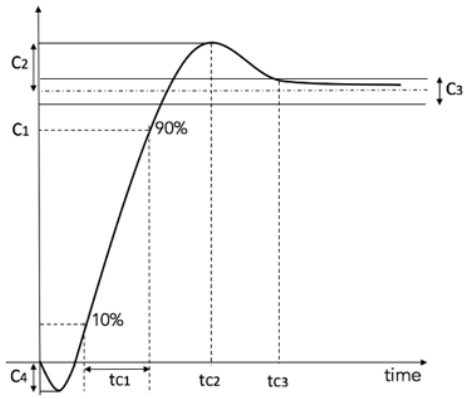

Figure 3. Response specifications for a step change.

IV. Results and Discussion

Unconstrained GPC controller does not include the rate-limit constraint at the guide vane, which is mandatory in the turbine governor applications. A fixed rate-limit, at which the guide vane can open or close, prevents excessive variations in the tunnel pressure and is necessary due to safety reasons. Additionally, this constraint plays a vital role in mitigating the NMP behavior, which occurs during the initial part of power transients. Due to these reasons, this section contains only the response produced by a constrained GPC controller, which is compared to the response produced by the PI controller. Two cases are analyzed. In the first case load/frequency controller does not have an obligation to provide primary reserve (load control mode), while in the second case obligation to provide primary reserve is included (frequency control mode). The step response specifications for single-unit operations, shown in Fig. 3, is used as a reference.

The three most important criteria that will be analyzed are the following:

- NMP undershoot,
- Overshoot,
- Primary response – at least 90% of demanded step power change realized within 10 s of initiation.

Table II shows that NMP response (C_4 criterion) must be under 2% and overshoot (C_2 criterion) must be below 4%.

The responses of the model introduced in Section II are given in Fig. 4 and Fig. 5, respectively. Load control mode is presented in Fig. 4, while frequency control mode is presented in Fig. 5. Black dotted line in both figures presents the response of the PI controller, while blue line is used to present the response of GPC controller. Simulated PI and GPC controller settings are given in Table III. The following GPC controller settings are defined in Table III: prediction horizon N, control horizon N_u and control weighting W_u. Aspects constituting a long prediction and control horizons are not explicitly defined and for every application may require the trial-and-error simulations. In this paper, the trial-and-error simulations result in minimum prediction horizon length $N = 40$, control horizon length $N_u = 10$ and control weighting $W_u = 150$. The parameters of the PI controller are defined in the way that the system has reasonable value of the gain margin ($2 \leq G_m \leq 5$) and the phase margin ($30^\circ \leq P_m \leq 60^\circ$) [16]. The gain and phase margin for the analysed system are given in Fig 6.

TABLE II
Specifications for the control design [15].

Criterion	Specification for single unit step response
C_1 - rise time	$C_1 \geq 90\%$ at $t_{C_1} = 10$ s
C_2 - overshoot	$C_2 \leq 4\%$ and $t_{C_2} \leq 15$ s
C_3 - settling time	$t_{C_3} = 30$ s for $C_3 \leq 0.5\%$
C_4 - NMP	$C_4 \leq 2\%$

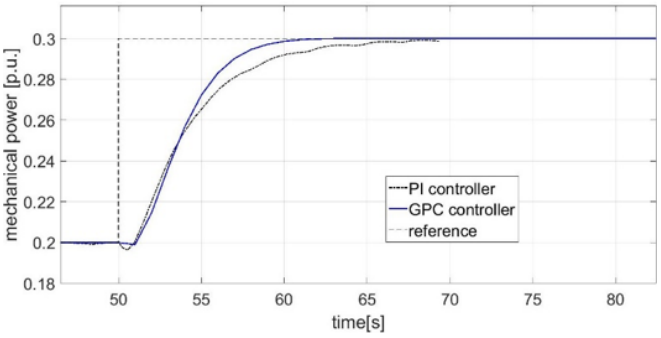

Figure 4. Comparison of step responses produced by the GPC and PI controllers – load control mode.

TABLE III
Controller settings.

Controller	Settings	
PI	$K_p = 0.017$	$K_i = 0.17$
GPC	$N = 40$	$N_u = 10$
	max $u = 1$ $p.u.$	min $u = 0$ $p.u.$
	max $\Delta u = 0.1$ $p.u.$	min$\Delta u = 0.01$ $p.u.$
	$W_u = 150$	

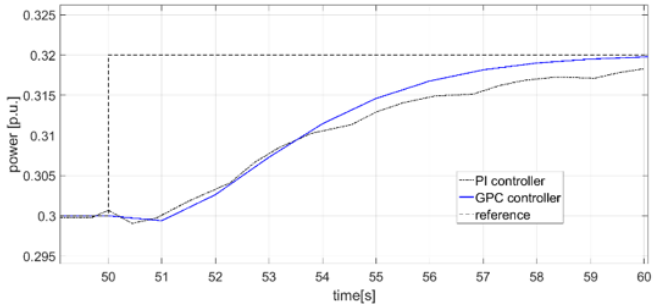

Figure 5. Comparison of step responses produced by the GPC and PI controllers – frequency control mode.

Structure of both models is presented in Fig. 2. Black line in Fig. 2. presents grid frequency measurement required in frequency control mode. Parameter D is used to introduce the droop characteristic. The value of D in the frequency control

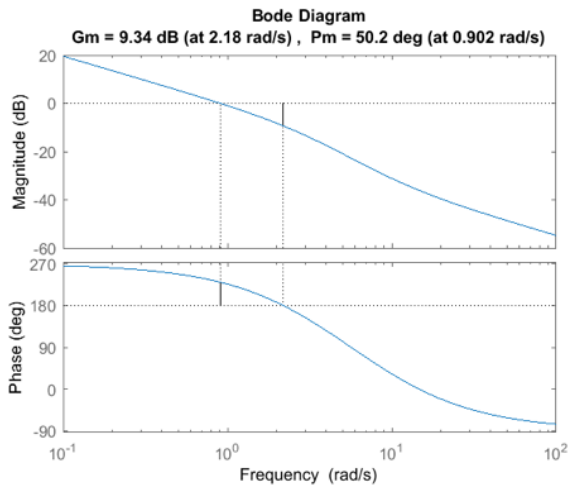

Figure 6. Stability margins.

mode is equal to 2%, which means that if grid frequency decreases by 1%, the hydropower plant will increase its power output by 2% to stop further frequency decrease.

Additionally, a comparison of PI and GPC responses using the criteria defined in Table II is shown in Tables IV and V.

TABLE IV
COMPARISON OF PI AND GPC RESPONSES – LOAD CONTROL MODE.

Criterion	PI	GPC
C_1	90% at 9.2 s	90% at 6.9 s
C_2	No overshoot	No overshoot
C_3	11.9 s	8.1 s
C_4	3.8%	1%

TABLE V
COMPARISON OF PI AND GPC RESPONSES – FREQUENCY CONTROL MODE.

Criterion	PI	GPC
C_1	90% at 9.8 s	90% at 7.1 s
C_2	No overshoot	No overshoot
C_3	11.2 s	7.5 s
C_4	3.4%	1.3%

In the first case, where load control mode is simulated, Unit 3 of hydropower plant Miljacka operates initially at 0.2 $p.u.$ of the full load. After that, a 0.1 $p.u.$ step demand (10% of the rated power) is applied to Unit 3. Fig. 4 and Table IV show that step response in load control mode with GPC controller settles 3.8 s sooner, NMP undershoot is reduced by 2.8% and primary response is 2.3 s faster than in the case with the PI controller.

In the second case, where automatic frequency control mode is simulated, Unit 3 of hydropower plant Miljacka operates initially at 0.3 $p.u.$ of the full load. At $t = 50$ s, a disturbance occurs and the grid frequency is decreased by 1%. Since the droop characteristic of Unit 3 is $D = 2\%$, active power reference trajectory is increased by 2% (0.02 $p.u$) to compensate for this frequency deviation. Fig. 5 and Table V show that response in the frequency control mode with GPC controller settles 3.7 s sooner, NMP undershoot is reduced by 2.1% and primary response is 2.7 s faster than in the case with the PI controller.

Additional simulations, presented in Fig. 7, are conducted with W_u values of 150, 100, 50 and 10. They show that it is possible to achieve faster GPC response by reducing the value of W_u, which penalizes the control effort. In this case, NMP undershoot and overshoot are increased, which means that further improvements are possible only at the expense of another criteria.

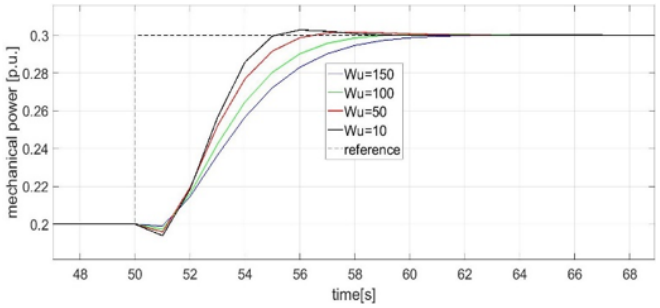

Figure 7. Influence of W_u on GPC response.

V. CONCLUSION

The main intention of this paper was to show the possibility of applying MPC controller as frequency/load controller in a turbine governor. A linearized SISO plant model was used for the simulation purposes and comparison between the standard PI and the MPC controller shows that predictive control strategy improves control behavior of a turbine governor. In Section IV, simulation results have shown that PI controller violates undershoot criterion, defined in Table II, while GPC controller satisfies all criteria and shows superiority over the classical PI controller.

Although the GPC controller simulations have shown promising results, it is still not clear whether this type of controllers have practical implementation potential due to implementation complexity and difficulty of industrial application of the predictive control. A new generation of turbine governor hardware is capable of dealing with computational requirements of prediction control, but to the best of the authors' knowledge, currently there is no practical implementation of the predictive control in the turbine governor applications. Therefore, further research will primarily be focused on the practical implementation of the predictive controller on a hydropower plant model available in the Smart Grid Laboratory at the University of Zagreb Faculty of Electrical Engineering and Computing. Furthermore, behavior of the MPC controller in presence of measurement noise and the influence of predictive control strategy on control activity of the plant will be investigated.

ACKNOWLEDGEMENT

This work has been supported in part by the Croatian Environmental Protection and Energy Efficiency Fund under project Microgrid Positioning – uGRIP, as well as by Croatian Science Foundation and Croatian TSO (HOPS) under project Smart Integration of RENewables - SIREN (I2583-2015).

REFERENCES

[1] J. Culberg, M. Negnevitsky, and K.A. Kashem, "Hydro-turbine governor control: theory, techniques and limitations", *in Australasian Universities Power Engineering Conference, (AUPEC 2006)*, 2006.

[2] ABB, "Hydro power - Intelligent solutions for hydro governors", 2016.

[3] C. Aurora, L. Magni, R. Scattolini, P. Colombo, F. Pretolani and G. Villa, "Predictive Control of thermal Power Plants", *International Journal of Robust and Nonlinear Control*, vol. 14, no. 4, pp.415-433, 2004.

[4] A. Y. Begum, and G. V. Marutheeswar, "Design of MPC for superheated steam temperature control in a coal-fired thermal power plant", *Indonesian Journal of Electrical Engineering and Computer Science*, vol. 4, no. 1, pp.73-82, 2016.

[5] O. Mohamed, J. Wang, A. Khalil, and M. Limhabrash, "Predictive control strategy of a gas turbine for improvement of combined cycle power plant dynamic performance and efficiency", *SpringerPlus*, vol. 5, no. 1, p.980, 2016.

[6] L. C. Henriksen, M. H. Hansen, and N. K. Poulsen, "Wind turbine control with constraint handling: a model predictive control approach", *Published in IET Control Theory and Applications*, vol. 6, no. 11, pp.1722-1734, 2012.

[7] L. C. Henriksen, N. K. Poulsen, and M. H. Hansen, "Nonlinear Model Predictive Control of a Simplified Wind Turbine", *Proceedings of the 18th World Congress The International Federation of Automatic Control*, vol. 44, no. 1, IFAC, 2011.

[8] B. Strah, "The water turbine regulation of adaption to faults in guide vane system", Master Thesis (in Croatian), University of Zagreb Faculty of Electrical engineering and Computing, 2000.

[9] P. Kundur, *Power System Stability and Control*, New York:McGraw-Hill, 1994.

[10] T. Tomisa, "Parameter Estimation of High Pressure Hydro-Electric Power Plant Conduit Hydraulic System", Doctoral Thesis (in Croatian), University of Zagreb Faculty of Electrical Engineering and Computing, 1995.

[11] Working Group on Prime Mover and Energy Supply Models for System Dynamic Performance Studies, "Hydraulic Turbine and Turbine Control Models for System Dynamic Studies", *IEEE Transactions on Power Systems,*, vol. 7, no. 1, pp.167-179, 1992.

[12] J. M. Maciejowski, *Predictive control: with constraints*, Englewood Cliffs, NJ: Prentice-Hall, 2002.

[13] E. F. Camacho and C. Bordons, *Model Predictive Control*, New York: Springer-Verlang, 1999.

[14] L. Wang, *Model Predictive Control System Design and Implementation Using MATLAB.*, Springer, 2009.

[15] K. J. Astrom and T. Hagglund, *PID controllers: theory, design and tuning.*, Instrument Society of America, Research Triangle Park, NC, 1995.

[16] K. J. Astrom and R. M. Murray, *Feedback Systems: An Introduction for Scientists and Engineers.*, vol. 36, no. 4. 2008.